

RAPID AND DYNAMIC DETECTION OF ANTIMICROBIAL RESPONSE OF  
PATHOGENIC BACTERIA USING MZO NANOSTRUCTURE-MODIFIED QUARTZ  
CRYSTAL MICROBALANCE

By

YIFAN WU

A thesis submitted to the

School of Graduate Studies

Rutgers, the State University of New Jersey

In partial fulfillment of the requirements

For the degree of

Master of Science

Graduate Program in Electrical and Computer Engineering

Written under the direction of

Yicheng Lu

And approved by

---

---

---

---

New Brunswick, New Jersey

May 2019

## ABSTRACT OF THE THESIS

Rapid and dynamic detection of antimicrobial response of pathogenic bacteria using MZO  
nanostructure-modified quartz crystal microbalance

by

YIFAN WU

Thesis Director:

Professor Yicheng Lu

Antimicrobial resistance (AMR) threatens the effective prevention and treatment of a constantly increasing range of infections caused by bacteria, parasites, viruses and fungi, and has caused a dramatic increase in infection-related deaths, such that it threatens to become the next world pandemic. We report a magnesium zinc oxide nanostructure (MZO<sub>nano</sub>) modified quartz crystal microbalance (QCM) biosensor for rapid and dynamic detection of AMR. The sensor consists of a QCM with MZO<sub>nano</sub> grown directly on the sensing electrode using metalorganic chemical vapor deposition (MOCVD). The MZO<sub>nano</sub> sensing surface offers high-sensitivity to various biological species through surface-wettability and morphology control. Combining advantages of MZO<sub>nano</sub> with the QCM dynamic impedance spectrum makes the biosensor well-suited for monitoring viscoelastic transitions during drug treatment compared to the conventional frequency shift signals from the QCM. Using the MZO<sub>nano</sub>-QCM, we demonstrated the dynamic real-time monitoring of culture growth and antimicrobial treatment effects on two clinically relevant bacterial strains: (1) Gram-positive strain *Staphylococcus epidermidis* and (2) Gram-

negative strain *Pseudomonas aeruginosa*. The antimicrobial treatment response of each of the two bacterial strains using Ciprofloxacin as the drug, was rapidly and dynamically detected. The standard microbiological protocols and assays were performed to determine the optimal drug dosages and the minimum inhibitory concentration to serve as the benchmark for the data reported by the sensors. The sensor also demonstrated capability to rapidly (within 1.5 hours) detect dosage dependent response of the two bacterial strains in real time. The testing results from two clinically-relevant bacterial strains mentioned above demonstrate the capabilities of the MZO<sub>nano</sub> - QCM to sense both mass accumulation and viscoelastic transitions during cell growth and drug treatment. It is found that the viscoelastic transitions of the bacterial cells during drug treatment gives higher sensitivity to the data as compared to the frequency shift signals of the device.

## Acknowledgements

*This work is supported by the*

***Rutgers TechAdvance™ Early Technology Development Fund.***

First, I would like to express my deepest appreciation to my advisor Prof. Yicheng Lu, for his kindness, support, inspirations in my research work. His great guidance, patience, and advice lead me to through smoothly understanding of my research. He consistently allowed this paper to be my own work but steered me in the right direction whenever I needed it.

I would also like to thank all experts who work with me on this project. I received tremendous help and understanding from them. I would like to thank Dr. Pavel Ivanoff Reyes who is not only the tutor for my research but also a good friend shared his experiences and idea for me. I would like to thank Mr. Guangyuan Li for helping me with the device fabrication and testing.

I would like to thank all the staff and co-workers in the Rutgers Public Health Research Institute (PHRI) Center. Especially thanks to Dr. Yuzhi Hong, and Prof. Xilin Zhao for their training and valuable advice in biological aspects on this research project.

I would like to thank my committee members, Prof. Yicheng Lu, Prof. Umer Hassan, and Prof. Chung-Tse Michael Wu for taking time and giving evaluations on my research work. Without them, I would not have been able to complete my master's thesis.

Finally, I would like to thank my parents and my boyfriend for their support and love to pursue my research.

## Table of Contents

<b>Abstract .....</b>	<b>ii</b>
<b>Acknowledgment .....</b>	<b>iv</b>
<b>List of Figures .....</b>	<b>vi</b>
<b>1. INTRODUCTION .....</b>	<b>1</b>
1.1. Antimicrobial Resistance .....	1
1.2. Bulk Acoustic Wave Devices .....	2
1.3. Magnesium Zinc Oxide and its Nanostructures.....	3
1.4. Objectives of the Thesis.....	4
<b>2. MATERIALS AND METHODS .....</b>	<b>6</b>
2.1. Fabrication of the MZO <sub>nano</sub> -QCM.....	6
2.2. Preparation of the Bacterial Cultures.....	7
2.3. Preparation of the Antibiotics .....	8
2.4. Dynamics and Kinetics Assays .....	8
<b>3. DEVELOPMENT OF MZO<sub>NANO</sub>-QCM BIOSENSOR .....</b>	<b>10</b>
3.1 Development and Optimization of the Sensor Device and Materials.....	10
3.2. Implementation of System Modeling and Data Analysis .....	12
3.3. Determination of Drug Treatment Dosage Factors.....	15
<b>4. DYNAMIC MONITORING OF MULTI-DOSAGE RESPONSE OF PAHTOGENIC BACTERIA</b> <b>.....</b>	<b>17</b>
4.1. Monitoring Drug Effects Using Standard Dynamics-Kinetics Assay .....	17
4.2. Dynamic Monitoring of Drug Effects Using MZO <sub>nano</sub> -QCM Biosensor.....	19
<b>5. CONCLUSION .....</b>	<b>25</b>
<b>References .....</b>	<b>28</b>

## List of Figures

**Fig. 1.** (a) MZO<sub>nano</sub>-QCM sensor device; (b) cross section schematic of the device structure. (c) FESEM image of the MZO nanostructures grown by MOCVD on the sensor electrode; (d) *S. epidermidis* bacterial growth on MZO nanostructures; and (e) *P. aeruginosa* bacterial growth on MZO nanostructures. **(Page 11)**

**Fig. 2.** (a) The mechanical impedance model of the nano-BAW cell monitoring system (b) the corresponding lumped-element equivalent circuit of the Butterworth-Van-Dyke (BVD). **(Page 12)**

**Fig. 3.** Screenshot of the implemented LabVIEW-based automation and data analysis module and software. **(Page 14)**

**Fig. 4.** (a) Results of the dynamics assay to determine the effective drug dosage of CIP antibiotic for the treatment of (a) *S. epidermidis* and (b) *P. aeruginosa*. **(Page 18)**

**Fig. 5.** Frequency shift from the sensor signal as a function of time for various CIP concentrations on (a) *P. aeruginosa* and (b) *S. epidermidis*. (Drug added at t=0) **(Page 21)**

**Fig. 6.** Motional resistance derived from the sensor impedance spectrum as a function of time for various CIP concentrations on (a) *S. epidermidis* and (b) *P. aeruginosa*. (Drug added at t=0). **(Page 24)**

## Chapter 1

### INTRODUCTION

#### 1.1 Antimicrobial Resistance

Antimicrobial drugs have greatly reduced infection-related illness and death; however, the extended use of antibiotics causes microorganisms to become adapted to these drugs through genetic alterations, giving rise to antimicrobial resistance (AMR). AMR threatens to become the next pandemic (World Health Organization 2014) and is becoming a major global-health concern according to the US Centers for Disease Control (CDC) [1]. Therefore, developing new technologies to dynamically and rapidly detect bacterial pathogens and ensure the most appropriate antibiotic choice early will drastically improve the timeliness and choice of antibiotic treatment [1]. However, the currently available conventional methods employed in screening antimicrobial susceptibility heavily rely on monitoring the growth of live microbial cells. The monitoring of the antimicrobial activity is typically handled through manually intensive assays and is time consuming (can take days even weeks for conclusive results). The currently available conventional laboratory methods employed in screening antimicrobial susceptibility and resistance include (i) viability counting on agar, (ii) determination of minimum inhibitory concentration (MIC) from broth dilution protocols, (iii) disk diffusion [2], including E-Test agar strips and (iv) optical density (OD) spectrophotometric techniques [3-4]. However, these testing methods are very slow and labor intensive and they also heavily rely on monitoring large amounts of live microbial cell cultures. The repetitive monitoring of the microbial culture is

typically handled under manual observation and assessment for further culturing or assaying. These periodic observations are time consuming, subjective, and require a large amount of samples in order to monitor the kinetics of growth of microbial cultures. Techniques such as surface plasmon resonance (SPR) spectroscopy and the surface-enhanced Raman scattering (SERS) spectroscopy have been developed to attempt rapid detection of antimicrobial susceptibility and resistance. SPR has been employed in the analysis of the binding mechanisms of cells [5-6]. SPR provides information on binding at the molecular level, and usually requires invasive tagging molecules (not label free). SERS has been applied to rapidly detect antibiotic susceptibility and resistance (within a few hours) by spectroscopic monitoring of the chemical changes to the cell wall of the bacteria [6]. However, both these spectroscopic methods require complicated and expensive optical measurement equipment and are not likely to be adopted into routine clinical use. Hence there is a compelling need for rapid and highly sensitive dynamic methods such as electronic biosensors to detect antimicrobial susceptibility for both effective treatment and discovery of drug resistance.

## **1.2 Bulk Acoustic Wave Devices**

Bulk acoustic wave (BAW) devices are typically composed of piezoelectric thin films sandwiched between two electrodes. Voltage signals applied across the electrodes cause acoustic wave resonance longitudinally along the bulk of the piezoelectric material making the device an efficient resonator. These BAW resonators have advantages, such as small size, low insertion loss, and lower power consumption. The quartz crystal microbalance (QCM) is a popular BAW device that has a high-quality factor, typically  $10^4$  to  $10^5$  at room temperature. It is a versatile research tool for chemistry, nanotribology,



wetting transition, and superfluid transition studies. QCM can operate in the range of several MHz to tens of MHz and have been used for mass detection. QCM sensors have also been used in biological applications such as adsorption of protein on metals [7], combined with ZnO nanostructures to detect DNA immobilization [8], and biological cell monitoring [9].

Acoustic impedance spectrum analysis from the BAW sensors through measurements of frequency shifts and temporal acoustic energy dissipation has been reported for dynamic cell monitoring using the QCM and the QCM with dispersion (QCM-D) biosensor [10-12]. Electrical impedance methods such as the microelectrode array [13] and the E-Plate impedance sensor [14-15] have been used to dynamically measure impedance changes of the sensor due to changes in cell activity. These techniques however are limited in sensitivity, especially for detection at early seeding stage of cell or bacterial growth. There is a need for a new BAW sensing technology with significantly higher sensitivity over these traditional devices.

### **1.3 Magnesium Zinc Oxide and its Nanostructures**

Magnesium zinc oxide (MZO) belongs to the oxide semiconductor family of materials under the zinc oxide (ZnO) category. Zinc oxide and MZO by extension is the 5th most abundant material on earth, and is emerging as a competitive alternative to silicon as a semiconductor material for microelectronic devices. ZnO is a wide bandgap ( $\sim 3.37$  eV at room temperature) semiconductor. With proper doping, ZnO and its nanostructures can be made into a multifunctional material that is particularly useful for sensing applications such as semi-conductivity, piezoelectricity, surface morphology tuning, wettability control,

and sensitivity to various biochemical and biological substances [16-21]. With a small composition (x) of Mg doping into ZnO, the formed  $\text{Mg}_x\text{Zn}_{1-x}\text{O}$  (MZO) essentially possesses all these properties of ZnO while having additional advantages of thermal stability [22] and large pH tolerance range during device fabrication and bio-testing process [23-24] in comparison with the pure ZnO. These properties of MZO and ZnO make this family of oxide nanostructures a promising biosensing material.

Recently, nanostructured ZnO ( $\text{ZnO}_{\text{nano}}$ ) has been used for biosensing applications; However, so far such applications have only been focused on (i) as a platform to facilitate cellular adhesion, (ii) as a conductive nano-coating for intracellular probes, and (iii) as a material for enhancing optical detection. By controlling the morphology of the ZnO nanostructured surfaces (thin film with flat, or rough surface, and nanotips), it can attach to certain biological cell lines (NIH 3T3 fibroblasts, umbilical vein endothelial cells, and capillary endothelial cells, etc) and control the extent of cellular adhesion [25]. ZnO nanostructures were also used to bind with bacterial and viral cultures for reaction with enzymes and antibodies for applications in immunosensing [26-27]. The use of ZnO nanorods as fluorescence enhancing substrates has been reported in [28].

## 1.4 Objectives of this Thesis

In this thesis, we aim to accomplish the following:

### (i) Develop the $\text{MZO}_{\text{nano}}$ -QCM biosensor:

We combine the enhanced sensing capability of the MZO nanostructures with the dynamic and real time capability of the QCM device to form the novel  $\text{MZO}_{\text{nano}}$ -QCM biosensor by directly depositing  $\text{MZO}_{\text{nano}}$  structures onto the top electrode of a QCM

device. The MZO nanostructured coating on the QCM serves as the biointerface nanomaterial which enables the high sensitivity feature of our biosensor. The high sensitivity of the biosensor is achieved because the nanostructured sensor surface provides very large effective sensing area available for the cell culture to cover, and the unique property of MZO nanostructures having controllable surface wettability, which significantly increases sample intake (cell number) for less sample volume.

**(ii) Utilize the MZO<sub>nano</sub>-QCM biosensor to monitor drug treatment response of two clinically relevant bacteria:**

The MZO<sub>nano</sub>-QCM biosensor is used for dynamic real-time monitoring of culture growth and antimicrobial treatment effects on the two clinically relevant bacterial strains: (1) Gram-positive strain *Staphylococcus epidermidis* and (2) Gram-negative strain *Pseudomonas aeruginosa* under various antibiotic dosage treatments. The dynamic and real-time monitoring feature of the MZO<sub>nano</sub>-QCM biosensor is enabled by the dynamic impedance spectrum capability of the QCM. The high sensitivity and rapid detection of drug susceptibility with various dosages are achieved.

## Chapter 2

### MATERIALS AND METHODS

#### 2.1 Fabrication of the MZO<sub>nano</sub>-QCM

The MZO<sub>nano</sub>-QCM sensor was fabricated by integrating the magnesium zinc oxide (MZO) nanostructures with the quartz crystal microbalance (QCM) (Fig. 1a-b). The MZO nanostructures were grown directly on the top electrode using metalorganic chemical vapor deposition using Diethylzinc (DEZn), MCp<sub>2</sub>Mg (bis-(methyl-cyclopentadienyl) magnesium) and ultra-high purity (99.999%) oxygen gas were used as the Zn metalorganic source, Mg metalorganic source and oxidizer, respectively. A small percentage amount of Mg doping into ZnO forms MZO, which decreases the Zn<sup>2+</sup> concentration in the cell medium by 4 times compared to the pure ZnO, lowering the toxicity of the sensor with the cell culture and prevents etching of the MZO film by acidic media [29]. The sensing surface is further modified by MZO nanostructures Fig. 1(c).

The operating frequencies of the standard QCM, and MZO<sub>nano</sub>-QCM were measured to be 10 MHz, and 9.912 MHz, respectively. All devices were sterilized and deployed inside a Teflon cell-growth wells and seeded with the bacterial cells. These were in turn placed inside a standard CO<sub>2</sub> incubator under controlled temperature at 37° C. The sensors were characterized using an HP 8573D Network Analyzer (Agilent Technologies, Palo Alto, CA), which were connected via IEEE-488 general purpose interface bus (GPIB) to the universal serial bus (USB) of a microprocessor running a data acquisition program. The acoustic transmission ( $S_{21}$ ) spectrum of the device was automatically measured and

digitally stored for a fixed monitoring interval during the microbial culture growth on the sensors inside the incubator. The output of the sensor devices was in the form of time-frequency set of signals. These signals were then analyzed by extracting the peak frequency shifts and impedance amplitude modulations experienced by the devices relative to their starting frequencies and amplitudes due to the mass change and viscoelastic transitions on the sensing surface.

## **2.2. Preparation of the Bacterial Cultures**

In order to demonstrate the dynamic real-time monitoring of the two clinically relevant bacterial strains using our sensor technology, we first performed standard culture growth protocols/assays and optimization of antimicrobial treatment effects on two clinically relevant bacterial strains: (1) Gram-positive strain *Staphylococcus epidermidis* and (2) Gram-negative strain *Pseudomonas aeruginosa*. *Staphylococcus epidermidis* ATCC 35984 was inoculated into Tryptic Soy Broth (TSB; Becton Dickinson) and *Pseudomonas aeruginosa* was inoculated into Mueller Hinton Broth (MHB; Becton Dickinson). Both bacterial strains were cultured at 37 °C for 16–18 h with shaking at 200 rpm. The stationary phase cultures of both strains were diluted 100-fold into fresh medium pre-loaded in 10-cm quad-plate petri dish, with each sector containing 5 ml cultures. The amount of cells in the diluted culture was determined by measurement of colony forming unit (CFU) on agar.

## **2.3. Preparation of the Antibiotics**

We explored the effect of various dosage (concentrations and treatment times) using Ciprofloxacin (CIP) as the antibiotic agent for both bacterial strains. The antibiotic

mentioned above was obtained from the hospitals at the Public Health Research Institute and Department of Microbiology, Biochemistry & Molecular Genetics, New Jersey Medical School, Rutgers University, Newark through the collaboration of Prof. Xilin Zhao. Various concentrations of the drug were used using dilution with distilled water as the solvent.

#### **2.4. Minimum Inhibitory Concentration (MIC) Determination**

The minimum inhibitory concentration (MIC) is the lowest concentration of an antibiotic that would cause the disappearance of visible colony growth of the targeted bacteria for a defined period of time [30]. The MIC is a standard measure for the degree of susceptibility of the targeted bacteria to the antibiotic treatment. Thus, drug treatment plans are expressed as a multiple of the MIC. The clinical standard in determining the MIC is through the broth microdilution technique. Cultures of *S. epidermidis* and *P. aeruginosa* at mid-log phase were diluted 1:1,000 in TSB or MHB broth to  $\sim 10^5$  CFU/mL. For each bacterial solution, 50  $\mu$ L of that solution was dropped in each micro-well a 100-well plate. Then, 12 different dilutions (successive two-fold dilutions) of the drug is introduced into the a well and incubated at 37 °C for 24 h. MIC was determined as the lowest antimicrobial concentration needed to inhibit culture growth, measured by turbidity, by at least 90% relative to an untreated control.

#### **2.5 Dynamics and Kinetics Assays**

Once the MIC of each drug was determined for each of the bacterial strains, we utilized the standard soft agar colony formation assay to use as a benchmark of the results

we obtained through the biosensor monitoring signals. To perform the Dynamics and Kinetics assay, we prepared multiple petri dishes coated with 0.25-inch-thick layer of soft agar (Sigma-Aldrich). We prepared a 1:200 diluted overnight bacterial culture and made 12 solutions for each of the three drugs used for that bacteria. The 12 solutions correspond to treatment of six different multiples of MIC of the drug (0 MIC, 1 MIC, 2 MIC, 4 MIC, 8 MIC, 16 MIC) for treatments of 1 hour, and 2 hours respectively. Each agar-coated petri dish is then inoculated with a 10  $\mu$ L drop of each of the six solutions and left overnight in a 37 °C incubator. The drops on the agar when left overnight should form white dots which are colonies of the bacterial strain that survived the drug treatment. The ratio of the colony forming units (CFU) for a particular MIC factor at a particular time over the CFU count with no treatment is called the survival rate. The plot of the survival rate vs the MIC multiple for each treatment time is called the Dynamics-Kinetics plot and signifies the drug response of the bacterial strain to a particular drug.

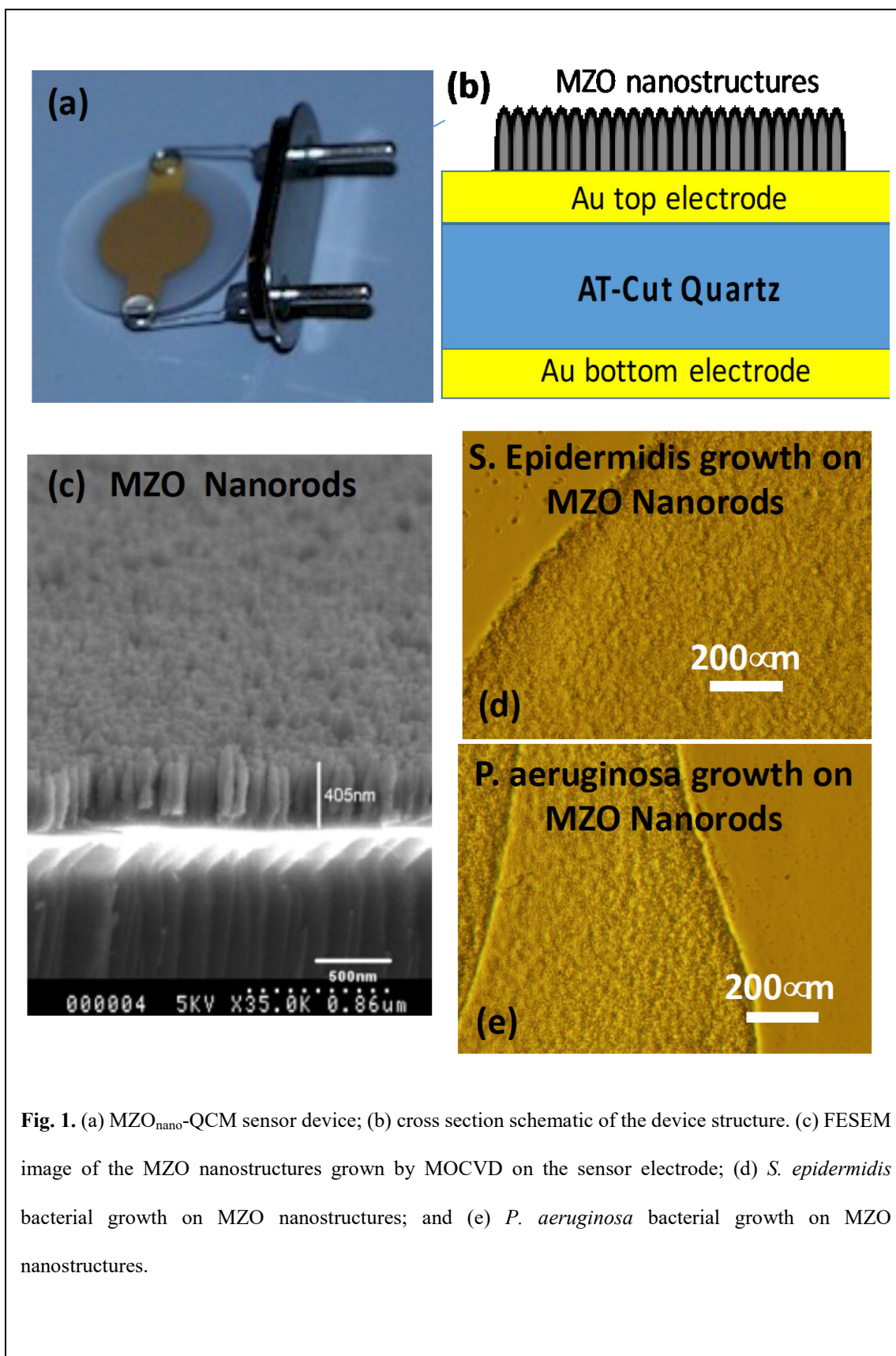
## Chapter 3

### DEVELOPMENT OF THE MZO<sub>NANO</sub>-QCM BIOSENSOR

#### 3.1 Development and Optimization of the Sensor Device and Materials

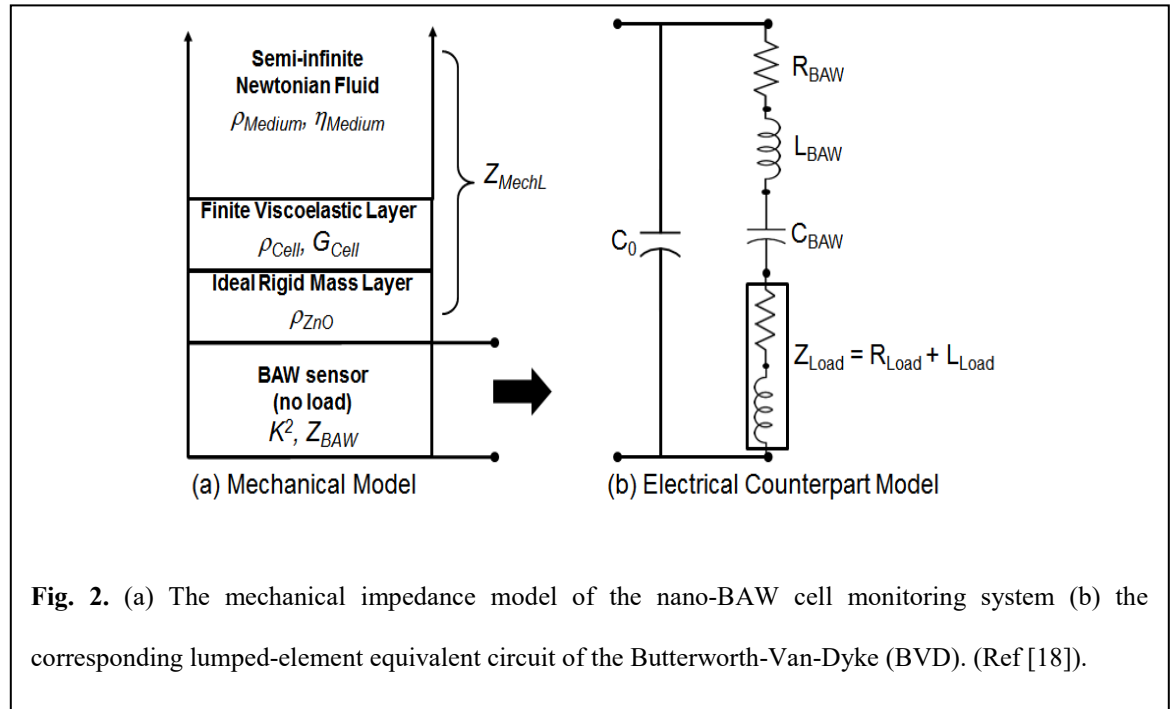
We have developed the MZO<sub>nano</sub>-QCM sensor by integrating the MZO nanostructures with the quartz crystal microbalance (QCM) (Fig. 1a-b). The MZO nanostructures were grown directly on the top electrode using metalorganic chemical vapor deposition using Diethylzinc (DEZn), MCp<sub>2</sub>Mg (bis-(methyl-cyclopentadienyl) magnesium) and ultra-high purity (99.999%) oxygen gas were used as the Zn metalorganic source, Mg metalorganic source and oxidizer, respectively. A small percentage amount of Mg doping into ZnO forms MZO, which decreases the Zn<sup>2+</sup> concentration in the cell medium by 4 times compared to the pure ZnO, lowering the toxicity of the sensor with the cell culture and prevents etching of the MZO film by acidic media. The sensing surface is modified by MZO with the proper morphology and wettability to enhance the cell growth compatibility and the sensitivity of the sensor. We cultured *Staphylococcus epidermidis* and *Pseudomonas aeruginosa* to evaluate their viability of strain growth on the MZO nanostructures. Fig. 1(c) shows the field emission scanning electron microscope image of the MZO nanostructures grown on the sensor surface. Fig. 1(d-e) shows the phase contrast microscopic images of the bacterial growth of *S. epidermidis* on MZO nanostructures. The results show that the MZO-nano morphology supports the cell growth.





### 3.2. Implementation of System Modeling and Data Analysis

The  $MZO_{\text{nano}}$ -QCM sensor signals are in the form of a single set of measurements of time-frequency 3D acoustic admittance spectra  $Y(t, \omega)$ , that contain in itself multiple parameters in a single monitoring period ((i) spectral shape evolution, (ii) peak frequency shift, (iii) Nyquist radius evolution, (iv) Nyquist rotation, and (v) motional impedance). These signals will give information about the biophysical properties of the cell culture.



We designed the system model and signal analysis module for the  $MZO_{\text{nano}}$ -QCM sensor. To establish direct correspondence between the BAW sensor measurements of  $Y(t, \omega)$  and mechanical changes to the cells, we adapted the transmission line model. The model of our bacterial cell monitoring system which consists of four mechanical transmission line impedance layers (Fig. 2(a)): (i) the basic BAW sensor at no load (ii) the surface-processed MZO nanostructure layer described by the ZnO density  $\rho_{\text{ZnO}}$ , (iii) the

biological cell layer described by the cell density  $\rho_{cell}$  and the complex shear modulus  $G_{cell}$ , and (iv) the cell growth medium modeled by its density  $\rho_{medium}$  and viscosity coefficient  $\eta_{medium}$ . This entire transmission line model can be collapsed into a lumped-parameter circuit equivalent called the Butterworth-Van-Dyke (BVD) lumped-parameter model [9, 31-32]. This assumption is valid for cell growth on BAW devices as the biological cells do not have very high viscosities and densities. The BVD equivalent circuit of the nano-QCM is shown in Fig. 2(b).  $Z_{Load}$  is the resulting motional impedance from perturbations contributed by the MZO nanostructure layer, cell growth layer, and the growth medium and are related by:

$$R_{Load} = \frac{\pi}{4K^2\omega_0 C_0} \frac{\text{Re}\{Z_{mechL}\}}{Z_{BAW}} = \frac{\text{Re}\{Y_{Load}\}}{\text{Re}^2\{Y_{Load}\} + \text{Im}^2\{Y_{Load}\}} \quad (1)$$

$$L_{Load} = \frac{\pi}{4K^2\omega_0 C_0} \frac{\text{Im}\{Z_{mechL}\}}{Z_{BAW}} = \frac{-\text{Im}\{Y_{Load}\}}{\omega_0 (\text{Re}^2\{Y_{Load}\} + \text{Im}^2\{Y_{Load}\})} \quad (2)$$

where  $K^2$  is the coupling coefficient of the piezoelectric layer,  $Z_{mechL}$  is the mechanical impedance due to the MZO nanostructure layer + cellular layer + growth medium attached to the basic BAW sensing area at no load  $Z_{BAW}$ . The quantity  $R_{Load}$  corresponds directly to the mechanical or motional resistance and designates dissipation of acoustic energy due to the attached cell growth layer on the MZO<sub>nano</sub>-TFBAR surface. The parameter  $L_{Load}$  on the other hand is directly proportional to the stored energy by the cell layer (i.e. elasticity increase).  $Y_{Load}$  is the measured admittance spectrum minus the no-load admittance spectrum of the BAW sensor. We designed the signal analysis procedure from the experiments in MZO<sub>nano</sub>-QCM testing devices. To eliminate the effects of the surface treated ZnO nanostructured layer and the cell growth medium, we separately monitored the

dynamic admittance spectra of the nanostructure layer and the growth medium for a period of time. Measurements of both layers do not contribute to the dynamic mechanical processes detected by the sensor and can be considered as background signals. After the background signals are subtracted, the output signals correspond solely to cellular activity. An automated signal measurement program was developed based on the LabVIEW software programming platform, and the implementation of the parameter extraction from the acoustic spectra of the sensor, and was utilized to obtain the experimental results from the sensor (Fig. 3).

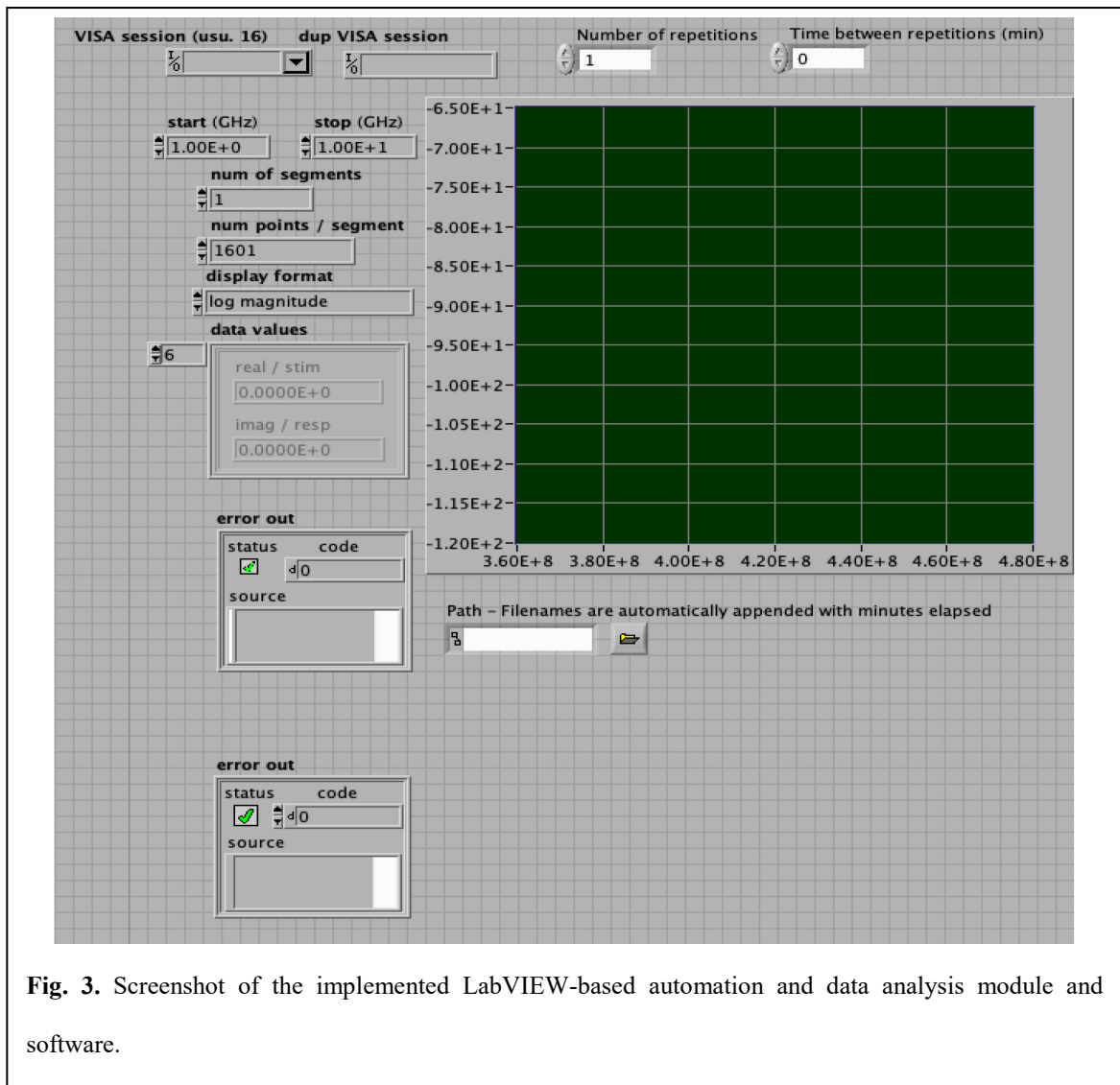


**Fig. 3.** Screenshot of the implemented LabVIEW-based automation and data analysis module and software.

The peak frequency shifts experienced by the device relative to their starting frequency due to the accumulation of mass on the sensing surface. According to Sauerbrey [33] the frequency shift of the impedance spectrum is directly proportional to the mass accumulation on the sensing electrode of the QCM by the expression:

$$\frac{\Delta f}{f_0} = \frac{2f_0}{v_q \rho_q A} \Delta m \quad (3)$$

where  $\Delta f$  is the frequency shift and  $f_0$  is the operating frequency of the device,  $v_q$  and  $\rho_q$  are the acoustic velocity and mass density of the AT-cut quartz layer,  $A$  is the sensing area of the top electrode, and  $\Delta m$  is the accumulated mass on the sensing electrode. We will show in the next chapter that both of these signal parameters:  $\Delta f$  and  $R_{\text{Load}}$  both give dynamic information regarding the drug response of both bacterial strains being investigated but that  $R_{\text{Load}}$  gives a significantly higher sensitivity to changes in the cell culture state during antibiotic treatments.

### 3.3. Determination of Effects of Drug Treatment Dosage on Bacteria Strain

In order to demonstrate the dynamic real-time monitoring of the initial two clinically relevant bacterial strains using our sensor technology, we first performed standard culture growth protocols/assays and optimization of antimicrobial treatment effects on two clinically relevant bacterial strains: (1) Gram-positive strain *Staphylococcus epidermidis* and (2) Gram-negative strain *Pseudomonas aeruginosa*. We explored **Ciprofloxacin (CIP)** as the antibiotic for each of the two bacterial strains.

We performed the broth micro-dilution standard assay to determine the minimum

inhibitory concentration (MIC) of CIP for the corresponding targeted bacteria. Using the MIC assay that was outlined in Chapter 2 we determined that Ciprofloxacin has a MIC of 0.05  $\mu\text{g/mL}$  for *S. epidermidis*, and MIC of 0.08  $\mu\text{g/mL}$  for *P. aeruginosa*. The MIC numbers will be the basis concentration to which the dosage dependent treatments will be derived from. We used the MIC values for the CIP antibiotic to determine the effective dosage for treatment of these two bacterial strains. The drug dosage is varied as a multiple of the MIC value.

## Chapter 4

### DYNAMIC MONITORING OF MULTI-DOSAGE RESPONSE OF PAHTOGENIC BACTERIA

#### 4.1 Monitoring Drug Effects Using Standard Dynamics-Kinetics Assay

We used the MIC values determined from the previous chapter for each of these antibiotics to determine the effective dosage for treatment of *S. epidermidis* and *P. aeruginosa* bacterial strains. The drug dosage is varied as a multiple of the MIC value. We performed the standard Dynamics-Kinetics Assay using the Colony Formation counting on soft agar plates as outlined in Section 2.4 to determine the colony survival rate as a function of MIC and treatment time. The results for the dynamics assay are shown in Fig. 4(a) for the drug response of *S. epidermidis* to CIP antibiotic, while Fig. 6(b) shows the drug response results of *P. aeruginosa* to CIP antibiotic. These drug response curves will be used to verify the results of the MZO<sub>nano</sub>-QCM in monitoring the same conditions.

Note that these drug susceptibility assays are highly labor intensive, very slow (takes 2 days to complete) and can only report colony formation unit CFU counts and requires large amounts of samples (~30 mL). Compared to these assays, our MZO<sub>nano</sub>-QCM requires < 2mL of samples, automatic (no user intervention needed), very fast and can report on cell count as well as biophysical transitions of the bacteria during drug treatment.

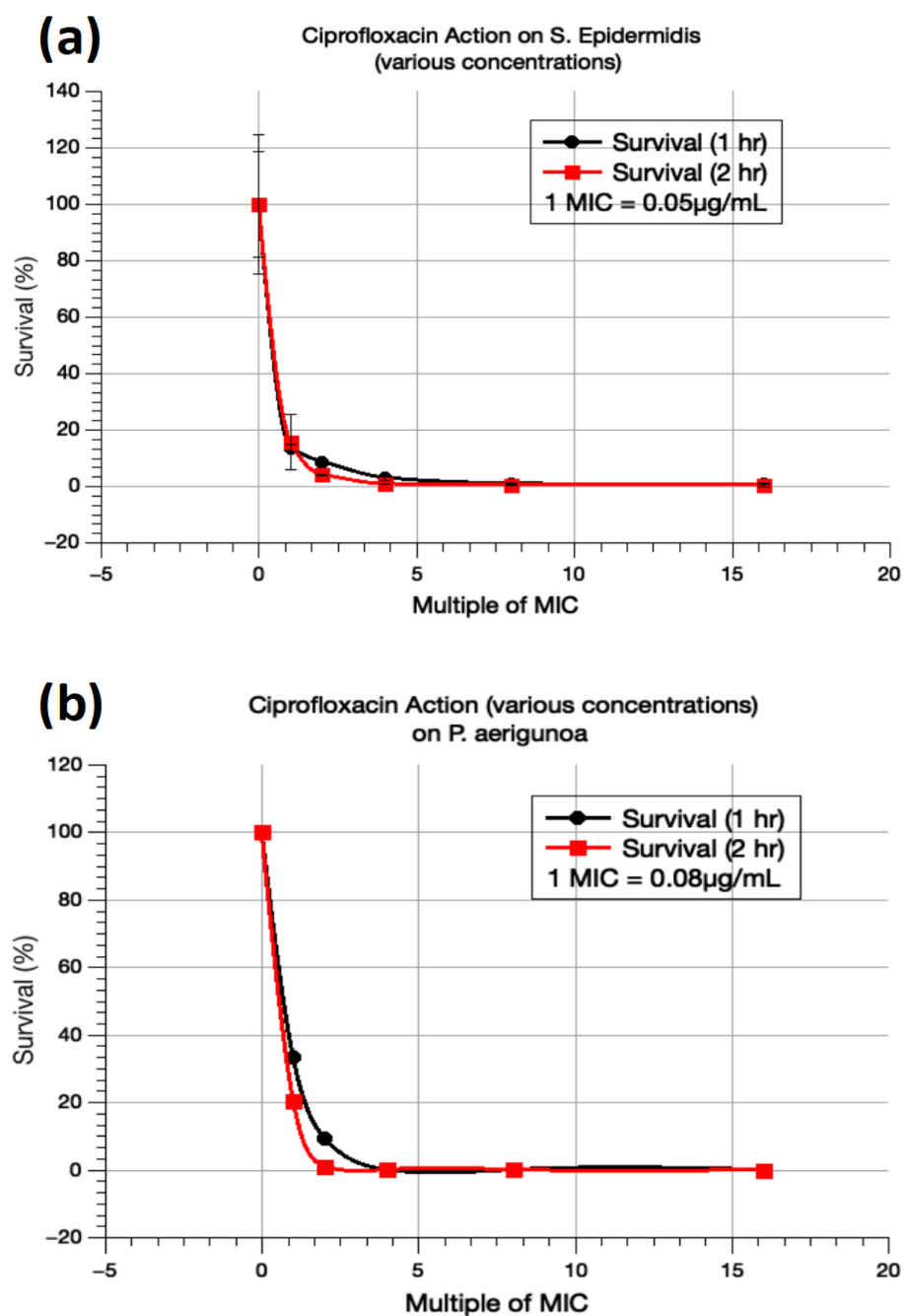


**Fig. 4.** (a) Results of the dynamics assay to determine the effective drug dosage of CIP antibiotic for the treatment of (a) *S. epidermidis* and (b) *P. aeruginosa*.



In Fig. 4(a) we see that for the CIP antibiotic, a 1-hr dosage is not enough to completely kill *S. epidermidis* if the concentration of the drug is less than 10MIC as shown by the survival rate values of the bacteria below the 10MIC dosages. For a 2-hr treatment, the drug can completely eradicate *S. epidermidis* for dosages above 5MIC. We can also conclude that Ciprofloxacin works as a good antibiotic to treat the *S. epidermidis* infection due to the low dosage and short timed treatment as it shows the dramatic decay of the survival rate at an earlier time and at a lower drug concentration. This is because we do not want to give a patient a very high dosage and long treatment of a drug because it might cause other health issues. Similarly, for *P. aeruginosa*, we can see that the same treatment response trend is seen for CIP used to kill this bacterium.

#### **4.2 Dynamic Monitoring of Antimicrobial Effects Using MZO<sub>nano</sub>-QCM Biosensor**

We demonstrated the dynamic real-time monitoring of culture growth and antimicrobial treatment effects on the two bacterial strains: *Staphylococcus epidermidis* and *Pseudomonas aeruginosa* using the magnesium zinc oxide nanostructure modified quartz crystal microbalance (MZO<sub>nano</sub>-QCM) biosensor that we developed and optimized as described in Chapter 3. We first performed the optimization of the bacterial inoculum seeding and drug dosage. Optimization of inoculum seeding and drug dosage dramatically improved test-to-control signal ratio for better detection resolution when we applied it to both bacterial strains and showed that the signal sensitivity dramatically increased. The sensor is then deployed in a standard incubator and connected to the network analyzer and data module.

The principal time-frequency acoustic impedance signals from the sensor provide multiple parameters that relate to biophysical properties of the bacterial strain culture as discussed in Chapter 3.

- The frequency shift  $\Delta f$  of the peaks of the acoustic spectrum is directly proportional to the mass accumulation on the sensor.
- Amplitude modulation of the impedance spectra indicate the stiffness of the accumulated strains on the sensor. The motional resistance ( $R_{\text{Load}}$ ) which is directly calculated from the two signals indicate cell stiffness and elasticity respectively (viscoelastic transitions of the cell culture). The viscoelastic transition monitoring is especially important in determining whether the sample in the sensor system is forming a normal cell culture or cell death due to drug effects.

The admittance spectrum ( $Y(f,t)$ ) of the sensors were continuously measured. We applied the multilayer-transmission-line Butterworth-Van-Dyke (BVD) model on  $Y(f,t)$  to measure motional resistance ( $R_{\text{Load}}$ ).  $R_{\text{Load}}$  corresponds directly to energy dissipation by the cell layer.

Fig. 5(a) shows the effects of ciprofloxacin on *P. aeruginosa* for various multiples of the minimum inhibitory concentration (MIC). The MIC for ciprofloxacin (0.08  $\mu\text{g/mL}$ ) on *P. aeruginosa* was obtained through the standard broth dilution assay. For monitoring the growth of *P. aeruginosa* and the subsequent drug effects using the MZO<sub>nano</sub>-QCM sensor, we seeded the sensor with a 2mL solution containing a 20-fold diluted *P. aeruginosa* culture under early-log phase and the ciprofloxacin of a particular MIC multiple. The sensor was placed inside an incubator at 37 °C while automatically measuring the acoustic

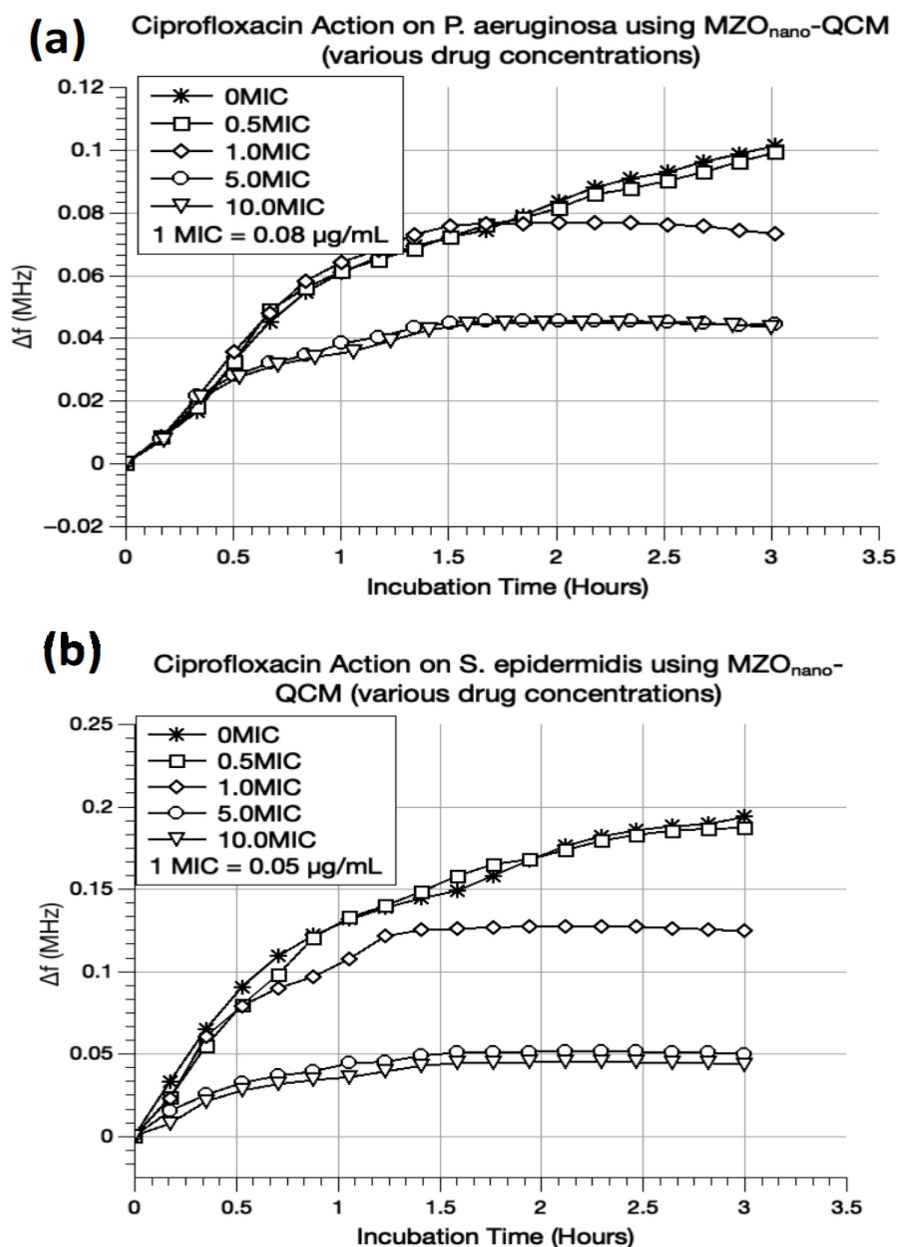


**Fig. 5.** Frequency shift from the sensor signal as a function of time for various CIP concentrations on (a) *P. aeruginosa* and (b) *S. epidermidis*. (Drug added at  $t=0$ ).

spectrum every 15 minutes for 3 hours. The peak frequency shift ( $\Delta f$ ) of the acoustic spectrum was computed and plotted as a function of time. For the no-drug condition (0 MIC), the  $\Delta f$  plot increased continuously for the entire duration of the monitoring period,

which corresponds to the mass accumulation of the growing bacteria. A similar pattern is observed for the sample that was treated with 0.5 MIC of ciprofloxacin, which indicates that the drug concentration is not enough to kill the bacteria. At 1 MIC, the plot starts to taper off and flatten at 1.5 hours, which is expected for the dosage of exactly at the minimum inhibitory concentration. However, as the drug concentration introduced to the sample reaches 5 MIC and 10 MIC, the bacteria grows slightly but never reaches the same level as the no-drug  $\Delta f$  values, which indicates that the antibiotic dosage is working to kill the bacteria.

Fig. 5(b) shows the effects of ciprofloxacin on *S. epidermidis* for various multiples of the minimum inhibitory concentration (MIC). The MIC for ciprofloxacin (0.05  $\mu\text{g/mL}$ ) on *S. epidermidis* was obtained through the standard broth dilution assay. Similar to that of *P. aeruginosa* in Fig. 8(a), for monitoring the growth of *S. epidermidis* and the subsequent drug effects using the MZO<sub>nano</sub>-QCM sensor, we seeded the sensor with a 2mL solution containing a 20-fold diluted *S. epidermidis* culture under early-log phase and the ciprofloxacin of a particular MIC multiple. The sensor was placed inside an incubator at 37° C while automatically measuring the acoustic spectrum every 15 minutes for 3 hours. The peak frequency shift ( $\Delta f$ ) of the acoustic spectrum was computed and plotted as a function of time Fig. 8(b). In the no-drug condition (0 MIC), the  $\Delta f$  plot increased continuously for the entire duration of the monitoring period, which corresponds to the mass accumulation of the growing bacteria. The same observation was obtained for the 0.5 MIC ciprofloxacin treatment, which indicates that the drug concentration is not enough to kill the bacteria. At 1 MIC, the plot starts to taper off and flatten at 1 hour, which is indicative of the behaviour of the cells under minimum inhibitory concentration. For the

cases of 5 MIC and 10 MIC dosages, the bacteria grow slightly but never reaches at the same level as the no-drug  $\Delta f$  values, which indicates that the antibiotic dosage is working to kill the bacteria.

The second signal mechanism that provides more sensitivity is the motional resistance which is directly calculated using the Butterworth VanDyck Model (BVD) indicates cell stiffness and elasticity (viscoelastic transitions of the cell culture) (Fig. 6(a-b)). The viscoelastic transition monitoring is especially important in determining whether the sample in the sensor system is forming a normal cell culture or experiencing biomechanical disintegration due to drug effects on either the cell wall or the DNA in the nucleus. These two signals are readily available from the sensor upon its measurement of the acoustic spectrum. The motional resistance actually complements the information provided by the frequency shift plot and gives more sensitivity to the sensor. Fig. 6(a-b) show that the motional resistance actually dramatically changes compared to the frequency shift in indicating drug effects on the bacterial strains while being monitored by the sensor (compare with results from the frequency shift signals). We can see that  $R_{Load}$  increases when the bacterial cells are growing indicating that there is a lot of resistance to movement when the cells are healthy and densely populated whereas  $R_{Load}$  decreases when the drugs start attacking the bacterial cells and start disintegrating, indicating that the cell population has become more elastic and less resistive to movement. The graphs also confirm that at 10MIC at 1-hr point, the drug has shown its potency to treat the infection of both bacteria.

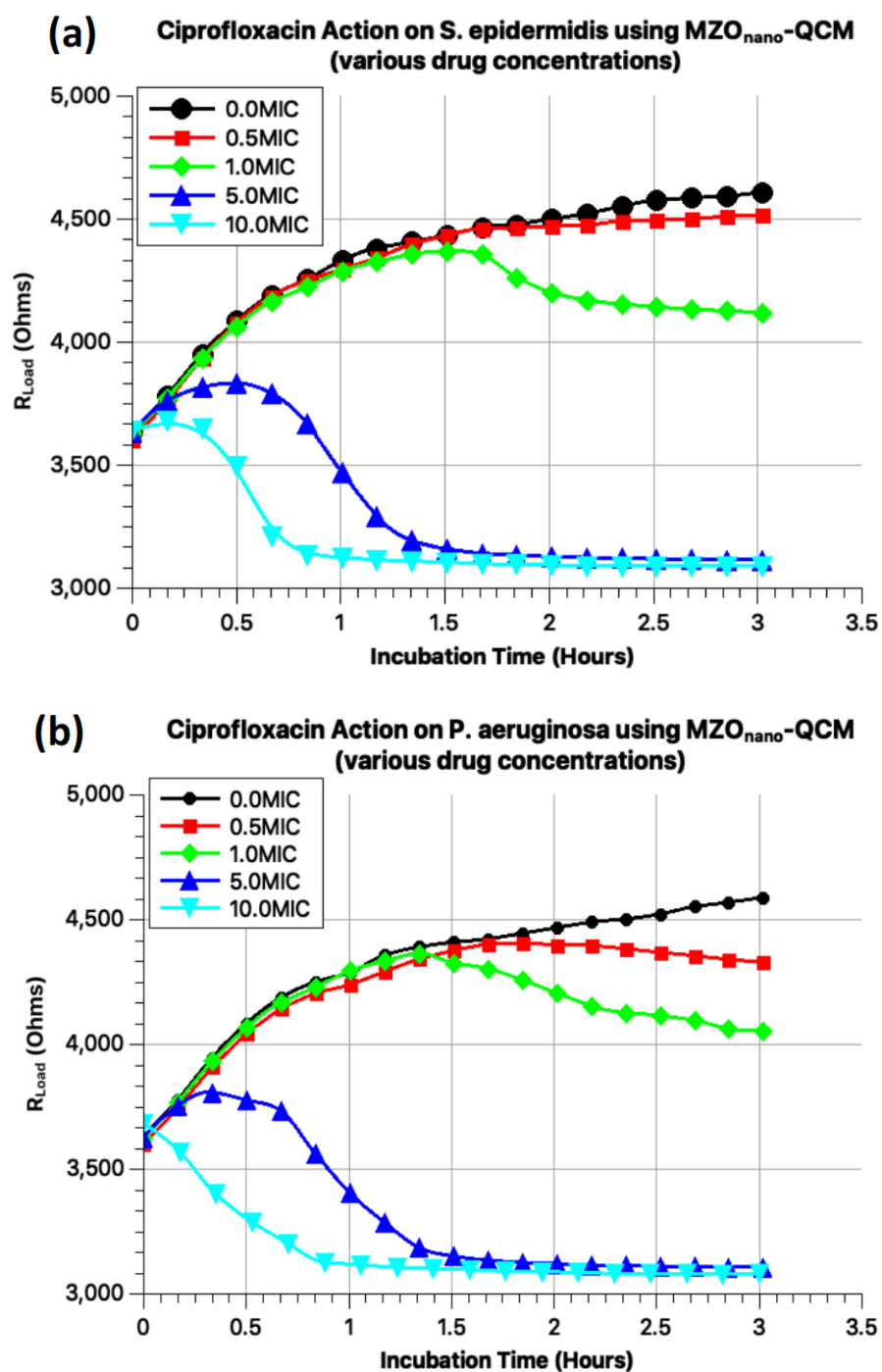


**Fig. 6.** Motional resistance derived from the sensor impedance spectrum as a function of time for various CIP concentrations on (a) *S. epidermidis* and (b) *P. aeruginosa*. (Drug added at  $t=0$ )

## CONCLUSION

### (i) Summary of Results

- We have developed the magnesium zinc oxide nanostructure modified quartz crystal microbalance (MZO<sub>nano</sub>-QCM) biosensor, which consists of a quartz crystal microbalance (QCM) with nano-MZO<sub>nano</sub> grown directly on the QCM sensing electrode. The MZO<sub>nano</sub> sensing surface morphology offers high-sensitivity to various biological species through surface-wettability and morphology control. Combining advantages of nano-MZO with the QCM dynamic impedance spectrum makes a highly-sensitive dynamic biosensor well-suited for monitoring viscoelastic transitions during drug treatment.
- The data analysis module was developed using the Butterworth-Van-Dyck (BVD) viscoelastic model for extraction of physical parameters from output signals coming from the MZO<sub>nano</sub>-QCM. The module also includes the automation of the signal measurements in addition to the data analysis. The module was implemented using a LabVIEW programming platform and Matlab coding of the BVD model.
- We have demonstrated the dynamic real-time monitoring of culture growth and antimicrobial treatment effects on two clinically relevant bacterial strains: (1) Gram-positive strain *Staphylococcus epidermidis* and (2) Gram-negative strain *Pseudomonas aeruginosa* using the magnesium zinc oxide nanostructure modified quartz crystal microbalance (MZO<sub>nano</sub>-QCM) biosensor. The antimicrobial (CIP) response of each of the two bacterial strains were rapidly and dynamically detected by the sensor. Standard microbiological protocols and assays were performed to determine the optimal drug

dosages and the minimum inhibitory concentration to serve as the benchmark for the data reported by the sensors.

- The sensor also demonstrated capability to rapidly (within 1.5 hours) detect dosage dependent response of the two bacterial strains in real time.
- The results on two clinically-relevant bacterial strains show capabilities to sense both mass accumulation and viscoelastic transitions during cell growth and drug treatment. The viscoelastic transitions of the bacterial cells during drug treatment are dynamically monitored by the motional resistance parameter that gives higher sensitivity to the data over the dynamics-kinetics broth dilution assays and the Klett suspension optical absorption methods.

## **(ii) Advantages and Significance**

Based on the results achieved to date, we have demonstrated highly sensitive, dynamic, rapid, compact and low-cost diagnostic sensor that non-invasively monitors bacterial cell behavior for antimicrobial susceptibility. Our biosensor measures bacterial cell count and biomechanical properties from its real-time signal spectra. The MZO nanostructured coating on the QCM serves as the biointerface nanomaterial which enables the high sensitivity feature of our biosensor. Also, due to the nature of the detection mechanism (mass accumulation and viscoelastic transitions), there is no need for biochemical labeling as an indicator (**label-free sensing**), and since the sensor deals with the monitoring directly on the cell culture, the monitoring procedure is non-invasive, which does not require complicated and labor-intensive pre-analysis preparation that standard assays require and significantly reduces sample volume requirement.



**(iii) Potential Applications**

The device enables to detect the transitory behavior of bacterial strains during normal growth and dosage dependent drug treatment. This technology could compete as a replacement for the standard labor-intensive MIC assays and resistance testing, including screening antibiotics for activity against resistant strains.

## Reference

1. Livermore, D., Blaser, M., Carrs, O., Cassell, G., Fishman, N., R. Guidos, R., Levy, S., Powers, J., Norrby, R., Tillotson, G., Davies, R., Projan, S., Dawson, M., Monnet, D., Keogh-Brown, M., Hand, K., Garner, S., Findlay, D., Morel, C., Wise, R., Bax, R., Burke, F., Chopra, I., Czaplewski, L., Finch, R., Livermore, D., Piddock L., White, T., 2011. *J. Antimicrob. Chemother.* 66, 9, 1941-1944.
2. Jorgensen, J., Turnidge, J., 2015. Susceptibility Test Methods: Dilution and Disk Diffusion Methods, in: Jorgensen J., Pfaller M., Carroll K., Funke G., Landry M., Richter S., Warnock D. (Eds.), *Manual of Clinical Microbiology*, Eleventh Edition. ASM Press, Washington, DC. doi: 10.1128/9781555817381.ch71, pp. 1253-1273.
3. Domingues, M.C., de la Rosa, M., Victoria Borobio, M., 2001. *J. Antimicrob. Chemother.*, 47, pp. 391-398.
4. Yourassowsky, E., Van der Linden, M. P., Lismont, M. J., Crokaert, F., & Glupczynski, Y. 1985. *Antimicrob Agents Chemother.*, 28, 6, pp. 756–760.
5. Giebel K.F., Bechinger C., Herminghaus S., Riedel M, Leiderer P., et al. 1999. *Biophys. J.* 76, pp. 509–16.
6. Chabot, V., Cuerrier, C., Escher, E., Almez, V., Grandois, Charette, P., 2009. *Biosens Bioelectron J.*, 24, pp. 1667-1673.
7. J. Homola, S. S. Yee, and G. Gauglitz, "Surface plasmon resonance sensors: review," *Sensors and Actuators B*, vol.54, pp.3, 1999.
8. X. C. Zhou, L. Q. Huang, and S. F. Y. Li, "Microgravimetric DNA sensor based on quartz crystal microbalance: comparison of oligonucleotide immobilization methods and the application in genetic diagnosis," *Biosensors & Bioelectronics*, vol.16, pp.85, 2001.
9. P.I. Reyes, Z. Duan, Y Lu, D. Khavulya, and N. Boustany, "ZnO Nanostructure-Modified QCM for Dynamic Monitoring of Cell Adhesion and Proliferation," *Biosensors and Bioelectronics* 41, pp. 84-89, Sept. 2012.
10. S. J. Braunhut, D. McIntosh, E. Vorotnikova, T. Zhou, K. A. Marx. *ASSAY and Drug Development Technologies*, Vol. 3 no. 1, pp 77-88, February 2005.
11. A. Alessandrini, M. A. Croce, and R. Tiozzo, P. Facci, "Monitoring cell-cycle-related viscoelasticity by a quartz crystal microbalance." *Applied Physics Letters*. vol. 88, February, 2006.
12. M. S. Lord, C. Modin, M. Foss, M. Duch, A. Simmons, F. S. Pedersen, B. K.

- Milthorpe, F. Besenbacher, "Monitoring cell adhesion on tantalum and oxidized polystyrene using a quartz crystal microbalance with dissipation," *Biomaterials*, 27, 4529-4537, 2006.
13. Huang, Xiaoqiu, D. W. Greve, D. D. Nguyen, and M. M. Domach. "Impedance based biosensor array for monitoring mammalian cell behavior." In *Sensors, 2003. Proceedings of IEEE*, vol. 1, pp. 304-309. IEEE, 2003.
  14. K. Solly, X. Wang, X. Xu, B. Strulovici, W. Zheng. "Application of Real-Time Cell Electronic Sensing (RT-CES) Technology to Cell-Based Assays" *ASSAY and Drug Development Technologies*, 2(4): 363-372, August 2004.
  15. Y. Abassi, "Label-free and dynamic monitoring of cell-based assays," *Biochemica*, no. 2, 2008, pp. 8-11
  16. Emanetoglu, N.W., Muthukumar, S., Wu, P., Wittstruck, R., Chen, Y., Lu, Y., 2003. *IEEE Trans. Ultrason, Ferroelec. Freq. Control*, 50, 5, 537.
  17. Reyes, P.I., Ku, C.J., Duan, Z., Lu, Y., Solanki, A., Lee, K.B., 2011. *Appl. Phys. Lett.* 98, 17, 173702.
  18. Reyes P.I., Duan Z., Lu Y., Khavulya D., Boustany N., 2013. *Biosens Bioelectron.*, 15, 41 pp. 84-89.
  19. Taratula, O., Galoppini, E., Wang, D., Chu, D., Zhang, Z., Chen, H., Saraf, G., Lu, Y., 2006. *J. Phy. Chem. B*, 110, 13, pp. 6506-6515.
  20. Zhang, Z., Emanetoglu, N. W., Saraf, G., Chen, Y., Wu, P., Zhong, J., Lu, Y., Chen, J., Mirochnitchenko, O., Inouye, M., 2006. *IEEE Trans. Ultrason. Ferroelect. Freq. Control*, 53, 4, pp. 786-792.
  21. Zhang, Z., Chen, H., Zhong, J., Saraf, G., Lu, Y., 2007. *J. Electron. Mater.* 36, 8, pp. 895-899.
  22. Ku, C.J., Duan Z., Reyes, P.I., Lu, Y., Xu, Y., Hsueh, C.L., Garfunkel E., 2011. *Appl Phys Lett.* 98, 12, pp. 123511.
  23. Chen, Y., Saraf, G., Lu, Y., Wielunski, L.S., Siegrist, T., 2007. *J. Vac. Sci. Technol A*, 25, 4, pp. 857.
  24. Brenner, T.M., Flores, T.A., Ndione, P.F., Meinig, E.P., Chen, G., Olson, D.C., Furtak, T.E., Collins, R.T., 2014. *J. Phys. Chem C*, 118, pp. 12599-12607.
  25. J. Lee, B.S. Kang, B. Hicks, T. Chancellor, Jr., B. Chu, W. Wang, B. Keselowsky, F. Ren, T. Lele, "The control of cell adhesion and viability by ZnO nanorods," *Biomaterials* 29 (2008) pp. 3743-3749.
  26. R. Yoshida, D. Kitamura, and S. Maenosono, "Mutagenicity of water-soluble ZnO nanoparticles in Ames test" *The Journal of Toxicological Sciences*, Vol. 34, No. 1, pp. 119-122, 2009.

27. Liu, J. Goud, P. M. Raj, M. Iyer, Z. Lin Wang and R. R. Tummala, "Real-time Protein Detection Using ZnO Nanowire/Thin Film Bio-sensor Integrated with Microfluidic System," 2008 Electronic Components and Technology Conference
28. Adam Dorfman, Nitin Kumar, and Jong-in Hahm, "Highly Sensitive Biomolecular Fluorescence Detection Using Nanoscale ZnO Platforms," *Langmuir* 2006, 22, 4890-4895
29. Brenner, T.M., Flores, T.A., Ndione, P.F., Meinig, E.P., Chen, G., Olson, D.C., Furtak, T.E., Collins, R.T., 2014. Etch-resistant Zn<sub>1-x</sub>Mg<sub>x</sub>O alloys: An alternative to ZnO for carboxylic acid surface modification. *J. Phys. Chem. C* 118, 12599–12607.
30. *Clinical Microbiology and Infection*, Volume 9 Number 8, August 2003, European Society of Clinical Microbiology and Infectious Diseases
31. H. Bandey, A. R. Hillman, M. J. Brown, and S. J. Martin, "Viscoelastic characterization of electroactive polymer films at the electrode/solution interface," *Faraday Discussions*, 107, pp 105-121, 1997.
32. J. Wegener, J. Seebach, A. Janshoff, and H-J. Galla, "Analysis of the composite response of shear wave resonators to the attachment of mammalian cells," *Biophysical Journal*, 78, pp. 2821-2833, June 2000.
33. G. Sauerbrey, English Translation of *Verwendung von Schwingquarzen zur Wagung dünner Schichten und zur Mikrowagung*, *Z. Phys* 155, 206 (1959).